



# Experimental evidence of synchronization in pulse-coupled oscillators with a refractory period and frequency distribution

Takuya Okuda, Keiji Konishi, and Hideki Kokame

Dept. of Electrical and Information Systems, Osaka Prefecture University  
 Email: {s0308okuda, konishi, kokame}@eis.osakafu-u.ac.jp

**Abstract**—In this paper, pulse-coupled oscillators with a refractory period and frequency distribution are investigated experimentally. The experimental results show that the stability condition of globally synchronization which was derived analytically in [Konishi and Kokame, 2008] is valid even for the experimental situations. In the case that the coupled oscillators have wide frequency distribution, the experimental results agree well with the analytical results. On the contrary, for narrow frequency distribution, there is a somewhat difference between the experimental and the analytical results. Our numerical simulations show that this difference would be reduced when the number of oscillators becomes large.

## 1. Introduction

In recent years, wireless sensor networks, which consists of a large amount of sensor nodes, have been intensively studied in the field of information and computer engineering [1]. In wireless sensor networks, each node gathers physical information around itself and communicates with each other. It is well known that there are some technical problems for practical implementation of the networks. The time synchronization of all the nodes is one of the important problems, since it plays crucial role on information integration. To overcome this problem, many researchers proposed the various rules [2]. Among those rules, pulse-coupled oscillators have been considered as one of the effective schemes [3].

For wireless sensor networks, a large amount of tiny sensor nodes are spatially distributed and the number of nodes changes from hour to hour. In such a situation, the following three specifications must be considered. First, each node is autonomous and they do not have an external electric power-supply. To extend its battery life, its power consumption must be reduced. Therefore, the communication time for each node should be shortened as much as possible. Second, since there are many sensor nodes in a network, they have to use standard popular-priced electronic devices in order to reduce hardware costs. Finally, time synchronization should be robust even if the number of sensor nodes changes one after another.

Synchronization in coupled nonlinear oscillators have been studied over many years [4, 5]. Mirollo and Strogatz reported that a globally pulse-coupled oscillators ex-

hibits synchronization for almost all initial conditions [6]. Since then, this type of network has been investigated for many situations: considering a frequency distribution [7], a refractory period [8], a local coupled network [9], and a transmission delay of the pulse signals [10]. In addition, an electrical circuit for a pulse-coupled oscillator was proposed [11].

For an applicative wireless sensor network, the pulse-coupled oscillators with a refractory period and frequency distribution, which take the three specifications into consideration, have been proposed in our previous study [12]. This study analytically provides the stability condition of global synchronization and the design for the idealized oscillators. However, we do not know whether our results are still valid for real oscillators or not. In order to confirm this, the present paper implements the pulse-coupled oscillator circuits, which are the modified circuits proposed in [11], and investigates their dynamics experimentally. These results are compared with the analytical results.

## 2. Pulse-coupled oscillators [12]

Let us consider a network of  $N$  oscillators. The phase of  $i$ -th oscillator is denoted by  $\phi_i(t) \in [0, 1]$  and developed by parameter  $\omega_i \in [\underline{\omega}, 1]$ , that is,

$$\frac{d\phi_i(t)}{dt} = \omega_i \quad (i = 0, 1, \dots, N-1). \quad (1)$$

The upper limit of  $\omega_i$  is set to 1 and the lower limit of it is set to  $\underline{\omega} \in (0, 1]$ . Let  $k \in \mathbb{Z}_+$  be the number of firings in the network. When the phase  $\phi_i(t)$  reaches 1 at time  $t^{k-}$ , the  $i$ -th oscillator fires and broadcasts a signal to all the other oscillators. Then, the phase  $\phi_i(t)$  is immediately reset to zero at time  $t^{k+}$ ,

$$\phi_i(t^{k-}) = 1 \Rightarrow \phi_i(t^{k+}) = 0. \quad (2)$$

At the same time,  $j(\neq i)$ -th oscillator being active,  $\phi_j(t^{k-}) \in [\delta, 1)$ , are forced to be reset to zero by the broadcast signal,

$$\phi_i(t^{k-}) = 1 \text{ and } \phi_j(t^{k-}) \in [\delta, 1) \Rightarrow \phi_j(t^{k+}) = 0, \quad \forall j \neq i. \quad (3)$$

On the contrary, the oscillators being sleep,  $\phi_j(t) \in [0, \delta)$ , are not reset,

$$\begin{aligned} \phi_i(t^{k-}) = 1 \text{ and } \phi_j(t^{k-}) \in [0, \delta) \\ \Rightarrow \phi_j(t^{k+}) = \phi_j(t^{k-}), \quad \forall j \neq i. \end{aligned} \quad (4)$$

For synchronization in these pulse-coupled oscillators, the following two stabilities are defined.

**[Local stability]** Suppose that the initial conditions of all the oscillators are

$$\phi_i(0) \in [\delta, 1], \quad \forall i \in \{0, 1, \dots, N-1\}. \quad (5)$$

The synchronization is said to be **locally stable** if all the oscillators have been synchronized since the first fire ( $n = 1$ ).

**[Global stability]** Suppose that the initial conditions of all the oscillators are

$$\phi_i(0) \in [0, 1], \quad \forall i \in \{0, 1, \dots, N-1\}. \quad (6)$$

The synchronization is said to be **globally stable** if all the oscillators have been synchronized since  $n$ -th fire.

It is obvious that initial condition (5) is included in condition (6). The design procedure which allows us to obtain locally stable and globally stable is given by the following two conditions.

**[Local stability condition]** If the lower bound of the parameter  $\underline{\omega}$  is greater than or equal to the refractory period  $\delta$ ,

$$\delta \leq \underline{\omega}, \quad (7)$$

then the synchronization is locally stable.

**[Global stability condition]** If the lower bound of the parameter  $\underline{\omega}$  and the refractory period  $\delta$  satisfy

$$\delta \leq g(n, \underline{\omega}), \quad (8)$$

$$g(n, \underline{\omega}) := \begin{cases} \frac{n-\sqrt{\underline{\omega}}}{1+n-\sqrt{\underline{\omega}}}, & (\underline{\omega} \geq \omega_n^*) \\ \underline{\omega}, & (\underline{\omega} \leq \omega_n^*) \end{cases}, \quad (9)$$

$$\omega_n^* := \left\{ \omega : \omega \in [0, 1), (1-\omega)^{n-1} = \omega^{n-2} \right\}, \quad (10)$$

then all the oscillators synchronize after at most  $n(\geq 2)$  fires for any initial condition.

It should be noted that inequality (8) is the sufficient condition of the global stability. Since the condition does not depend on the number of oscillators  $N$ , it is valid even for  $N \rightarrow \infty$ . For small  $N$ , we may obtain the globally stable synchronization even when inequality (8) is not satisfied. This fact will be discussed in Section 4.

### 3. Oscillator circuits

This paper provides the pulse-coupled oscillator circuits as shown in Fig. 1. The  $i$ -th oscillator circuit is governed by the circuit equation,

$$\frac{dV_i}{d\tau} = \begin{cases} \lambda_i(V_C - V_i), & kT_i \leq \tau < kT_i + t_{\lambda_i} \\ -\gamma_i V_i, & kT_i + t_{\lambda_i} \leq \tau < (k+1)T_i \end{cases}, \quad (11)$$

where

$$\lambda_i := \frac{1}{(R_{\lambda} + R_{\gamma})C_i}, \quad \gamma_i := \frac{1}{R_{\gamma}C_i},$$

$$t_{\lambda_i} := (R_{\lambda} + R_{\gamma})C_i \ln 2, \quad t_{\gamma_i} := R_{\gamma}C_i \ln 2,$$

$$T_i := t_{\lambda_i} + t_{\gamma_i} = (R_{\lambda} + 2R_{\gamma})C_i \ln 2.$$

The variable  $V_i$  is the voltage across capacitor  $C_i$  of the  $i$ -th circuit.  $\tau$  is the actual time.  $V_C$  is the power supply voltage. The period  $T_i$  equals the sum of the charging period  $t_{\lambda_i}$  and the discharging period  $t_{\gamma_i}$ . These periods depend on the resistors  $R_{\lambda} = 100$  [k $\Omega$ ] and  $R_{\gamma} = 3$  [k $\Omega$ ]. The comparator LM311 operates to switch the two states, sleep and active. The bias voltage  $V_{DD}$  of the comparator corresponds to the refractory period  $\delta$  in oscillators (1). Further, due to the operation of NE555, the voltage  $V_i$  wanders within the range  $V_i \in [V_C/3, 2V_C/3]$  (see Fig. 2).

The six ( $N = 6$ ) oscillator circuits, which are globally coupled by photo couplers, are implemented as shown in Fig. 1. The circuits are made up of standard popular-priced electronic devices. In general, although resistors have high degree of accuracy, capacitors have an error margin of tens of percents. The errors in capacitors inevitably cause the frequency distribution. Thus, in order to take the distribution into consideration, we explicitly deal with the error margin of capacitors. Throughout this paper, all of the capacitances are assumed to be within a range,  $C_i \in [C_{\min}, C_{\max}]$  for any  $i$ .

### 4. Experimental results

The previous paper [12] analytically provided the global stability condition (8) ~ (10), which depends on the refractory period  $\delta$  and the error range  $\underline{\omega}$ . The present paper shall confirm the analytical results by circuit experiments with

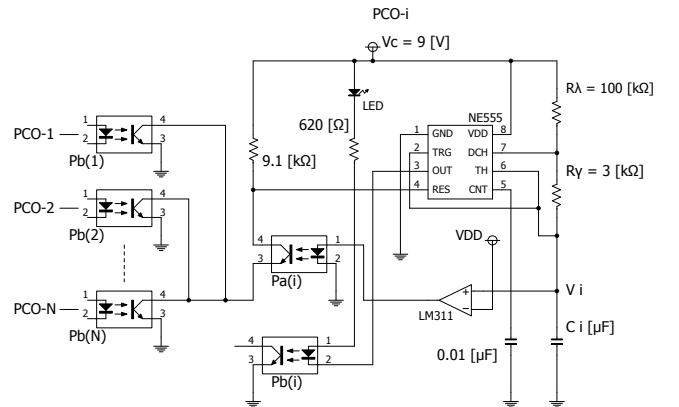


Figure 1: Pulse-coupled oscillator circuits.

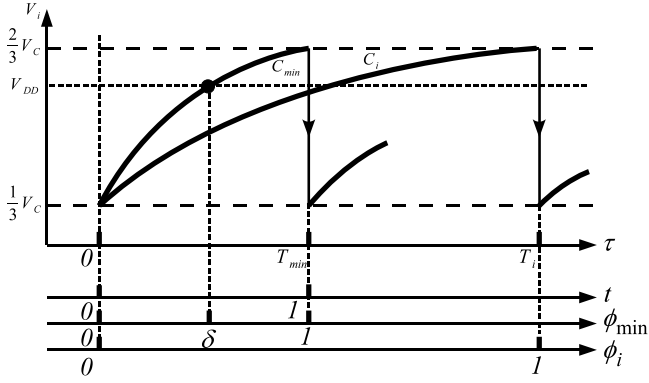


Figure 2: Relation between the voltage  $V_i$  and the phase  $\phi_i$ .

the following parameters:

$$V_C = 9 \text{ [V]},$$

$$C_{\min}/C_{\max} \in \{0.108, 0.215, 0.329, 0.438, 0.516, 0.583, 0.666, 0.757, 0.841\}.$$

The phase of the  $i$ -th oscillator,  $\phi_i(t)$ , corresponds to the voltage  $V_i$  of the  $i$ -th circuit. Their differences are summarized as follows. (i)  $V_i$  decreases along the discharging curve;  $\phi_i$  is immediately reset to zero. (ii)  $V_i$  increases along the charging curve;  $\phi_i$  increases linearly. The resistors governing the charging and discharging curves are set as  $R_\gamma \ll R_\lambda$ . Thus, the discharging period is very short compared with the charging one; then, it can be ignored. As a result, we can leave difference (i) out of consideration (see Fig. 2). Furthermore, we notice that difference (ii) can be also ignored by the rescaling,

$$\phi_i := \left\{ \ln \frac{2V_C}{3(V_C - V_i)} \right\} / \ln 2, \quad \omega_i := \frac{C_{\min}}{C_i},$$

$$t := \frac{\tau}{R_\lambda C_{\min} \ln 2}, \quad \underline{\omega} := \frac{C_{\min}}{C_{\max}},$$

$$\delta := \left\{ \ln \frac{2V_C}{3(V_C - V_{DD})} \right\} / \ln 2.$$

This rescaling indicates that circuits (11) are transformed into oscillators (1). Therefore, circuits (11) are dynamically equivalent to oscillators (1). From the above rescaling, global stability condition (8) ~ (10) can be also transformed into the following condition:

$$V_{DD} \leq \bar{V}_{DD}(n, C_{\min}/C_{\max}), \quad (12)$$

where the upper limit of  $V_{DD}$  is denoted by

$$\bar{V}_{DD}(n, C_{\min}/C_{\max}) := V_C \left( 1 - \frac{2}{3} e^{-g(n, \frac{C_{\min}}{C_{\max}}) \ln 2} \right). \quad (13)$$

Figure 3 shows that the global stability region on the  $C_{\min}/C_{\max} - V_{DD}$  plane. The solid line represents the

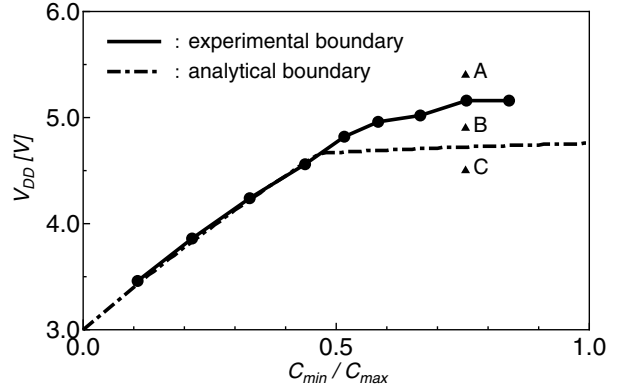


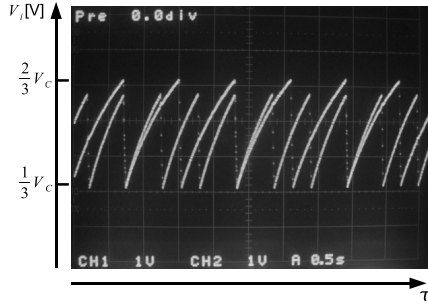
Figure 3: Global stability region in the  $C_{\min}/C_{\max} - V_{DD}$  space.

boundary of globally stable synchronization, which is obtained experimentally. When  $V_{DD}$  is set over the boundary (e.g., A in Fig. 3), the six circuits are not synchronized. Figure 4(a) shows the voltage  $V_i$  of the circuits whose parameters are set to point A in Fig. 3. It can be seen that the circuits are not synchronized. On the contrary, for  $V_{DD}$  under the boundary (e.g., B and C in Fig. 3), all of the six circuits are synchronized even when various external disturbances are applied to the circuits (see Figs. 4(b) and 4(c)).

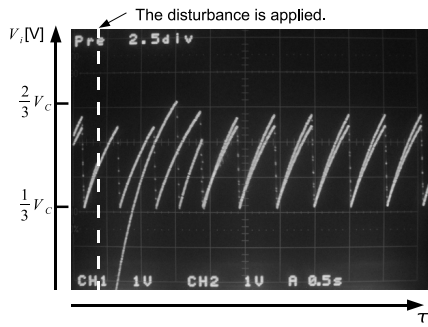
The dashed line in Fig. 3 represents the analytical boundary of globally stable synchronization,  $\bar{V}_{DD}$ , given by Eq. (13) with  $n = 7$ . This line indicates that if  $V_{DD}$  is set under the line, an arbitrary number of circuits are synchronized after at most seven fires. From the analytical results, we notice the following two facts: 1) Coupled circuits at points A and B in Fig. 3 do not satisfy the global stability condition; 2) Coupled circuits at point C satisfy the global stability condition. There is a somewhat difference between the solid line and the dashed line for the range  $C_{\min}/C_{\max} > 0.5$ . The difference is supposed to be caused by the following reason: although the solid line is based on our experiments of the six circuits, the dashed line is the boundary of the sufficient condition which does not depend on the number of circuits. Thus, our experimental results do not contradict the above facts.

In order to investigate the relation between the boundary and the number of circuits, we numerically estimate the boundary of globally stable synchronization on computer simulations. Figure 5 shows the boundaries with  $N = 3, 9, 20$ . As can be seen from this figure, the boundaries converge on the analytical one when  $N$  becomes large. Then, we notice that the solid line in Fig. 3 would converge on the dashed line when the number of circuits becomes large.

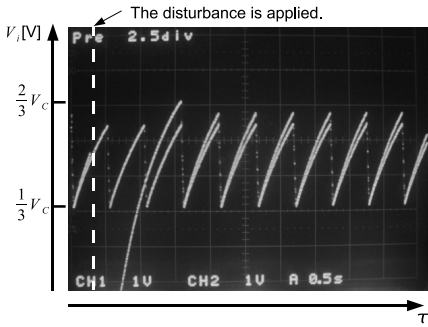
Inequality (12) is the sufficient condition of the globally stable synchronization, which does not depend on the number of circuits. Since the condition is valid for any  $N > 0$ , it



(a) Point A:  $V_{DD} = 5.40$  [V]



(b) Point B:  $V_{DD} = 4.90$  [V]



(c) Point C:  $V_{DD} = 4.50$  [V]

Figure 4: Time series data of voltage  $V_i$  ( $C_{min}/C_{max} = 0.756$ ).

is conservative for the small number of oscillators. In fact, for small  $N$ , we numerically obtain the globally stable synchronization even if inequality (8) is not satisfied (see Fig. 5).

## 5. Conclusion

In this paper, the pulse-coupled oscillators with a refractory period and frequency distribution have been investigated experimentally. The experimental results have shown that the stability condition of global synchronization is valid even for the experimental situations.

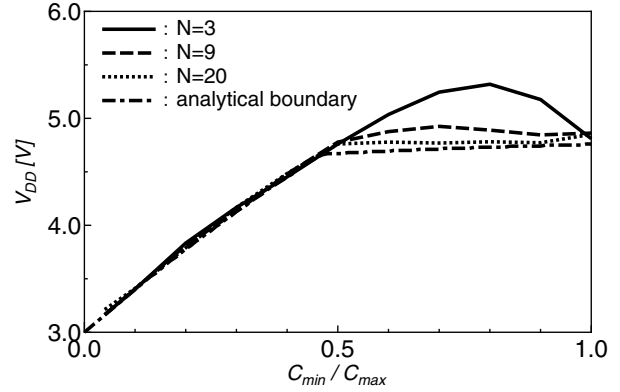


Figure 5: Boundaries of globally stable synchronization numerically estimated with  $N = 3, 9, 20$ .

## References

- [1] J.M. Kahn, R.H. Katz and K.S.J. Pister, *ACM/IEEE Intl. Conf. on Mobile Computing and Networking*, pp. 271–278, 1999.
- [2] F. Sivrikaya and B. Yener, *IEEE Network*, vol. 18, pp. 45–50, 2004.
- [3] Y. W. Hong and A. Scaglione, *IEEE Journal on selected areas in communications*, vol. 23, pp. 1085–1099, 2005.
- [4] T. Endo and S. Mori, *IEEE Trans. Circuits and Systems*, vol. 23, pp. 100–113, 1976.
- [5] Y. Nishio and A. Ushida, *IEEE Trans. Circuits and Systems-I*, vol. 42, pp. 678–686, 1995.
- [6] R.E. Mirollo and S.H. Strogatz, *SIAM Journal on Applied Mathematics*, vol. 50, pp. 1645–1662, 1990.
- [7] M. Tsodyks, I. Mitkov and H. Sompolinsky, *Phys. Rev. Lett.*, vol. 71, pp. 1280–1283, 1993.
- [8] C.C. Chen, *Phys. Rev. E*, vol. 49, pp. 2668–2672, 1994.
- [9] S. Bottani, *Phys. Rev. Lett.*, vol. 74, pp. 4189–4192, 1995.
- [10] W. Gerstner, *Phys. Rev. Lett.*, vol. 76, pp. 1755–1758, 1996.
- [11] G.M. Ramirez Avila, J.L. Guisset, and J.L. Deneubourg, *Physica D*, vol. 182, pp. 254–273, 2003.
- [12] K. Konishi and H. Kokame, *Chaos*, vol. 18, pp. 033132, 2008.